NUMERICAL DESIGN OF A COMPACT TE11-TO-TM01 MODE CONVERTER FOR THZ-DRIVEN ELECTRON ACCELERATION*

M. Kellermeier†, R. W. Assmann[1], T. Vinatier,
Deutsches Elektronen-Synchrotron DESY, Germany
W. Hillert, Universität Hamburg, Hamburg, Germany
[1] also at Istituto Nazionale di Fisica Nucleare, Frascati, Italy

Abstract

In recent years the generation of high power millimeter wave and Terahertz radiation has progressed substantially, enabling electron beam manipulation and acceleration in structures with a footprint of several centimeters. However, in many experiments the external driving pulse is coupled collinearly into the waveguide structure which increases the coupling footprint relative to the wavelength tremendously ($\approx 30\,\lambda$ or more) in comparison to conventional structures ($\approx 1\,\lambda$ or less). Here, the design of a double-bend mode converter for 300 GHz is presented which converts the fundamental TE_{11} mode quasi-instantaneously to the TM_{01} mode for the accelerating structure. In comparison to an *s-shaped* converter, the present design makes an additional waveguide bend obsolete. The structure length along the beam axis is only 4 mm ($4\,\lambda$), showing a major advance in compactness. Combined with a horn antenna for free-space to waveguide coupling, the maximum power coupled into the structure reaches 83 %, while the collinear scheme does not exceed 74 %.

INTRODUCTION

Since its first demonstration [1], THz- and millimeterwave driven electron acceleration and beam manipulation have made major progress due to emerging laser- or gyrotron-based high-power sources, promising higher field gradients and smaller footprint compared to conventional RF-driven structures [2–4]. This led to the initiation of the TWAC project (Terahertz wave accelerating cavity) [5] which aims for a compact high-peak current ($\approx$1 kA) accelerator, combining a conventional S-band RF gun with a THz-driven dielectric loaded waveguide (DLW) [6] for acceleration up to 10 MeV.

However, the THz beam is often coupled into the accelerating structure collinearly with the electron beam, which requires at least sufficient space for THz focusing. Further, the radially polarized Gaussian beam required to match the TM_{01} couples less efficiently ($\leq$83 %) to a conical horn antenna than the linearly polarized beam ($\leq$89 %). For a compact layout with high coupling efficiency, it may be beneficial to couple the linearly polarized THz beam to the TE_{11} waveguide mode, and further couple to the DLW under 90°. While 90° couplers are commonly used for conventional RF structures, they rely on a resonance for transferring the power into the TM_{01} mode.

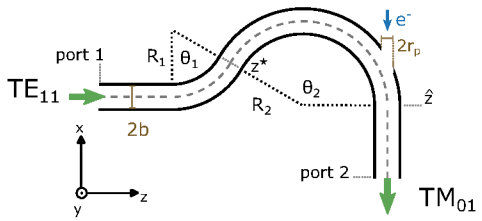

Figure 1: Parameterized hook-shaped double bend mode converter for TE_{11}–to–TM_{01} conversion.

Here, to achieve non-resonant, non-collinear coupling to the accelerating mode, bent circular waveguides are studied which transfer power from mode to mode via curvature [7–10]. While full power conversion cannot be obtained with a single bend [10], two bends with opposite sign of curvature enable full wave conversion. In many contexts the angles of the arcs are chosen such that the input and output planes are almost parallel [2, 11–13]. However, these *s-shaped* designs do not leave sufficient space for electron beam injection. In this work, the angle between input and output port is fixed to 90°. In contrast to the SLAC-110 GHz coupler [2, 14, 15], no additional waveguide bend is required. The structure is purely metallic since the dielectric loading is only required in the accelerating structure.

ANALYTICAL TWO-MODE MODEL

The *hook-shaped* geometry of the bend mode converter is illustrated in Fig. 1, in which $r_p = 0$ is set initially for pure mode conversion. The two arcs are characterized by their radius of curvature and the bending angle, with the constraint $\theta_1 + \theta_2 = -90°$ and $\theta_1 > 0, \theta_2 < 0, R_1 > 0, R_2 < 0$ by convention. The output power at port 2 is computed with the analytic two-wave model [10]. This model assumes that only the first two modes are propagating, and higher order modes are suppressed. Here, amplitude $A_1(z)$ refers to the fundamental TE_{11}, while $A_2(z)$ represents the TM_{01} mode of interest for acceleration. Perfect electric conductors walls are assumed. To solve the coupled mode equation a curvilinear coordinate system is used in which the unit vector $\mathbf{e}_z$ is tangential to the bend cylinder axis.

* Work supported by the European Research Council under the European Union's Seventh Framework Programme (FP/2007-2013)/ERC Grant No. 609920, and partially funded by the European Innovation Council (EIC) under the framework Horizon-EIC-2021-PathfinderOpen-01 (Grant agreement n. 101046504). Views and opinions expressed are however those of the author(s) only and do not necessarily reflect those of the European Union or EISMEA. Neither the European Union nor the granting authority can be held responsible for them.

† max.kellermeier@desy.de

Table 1: Geometric Parameters of the bend mode converters optimized for a frequency of 300 GHz, based on the analytical model and S-parameter simulations. The resulting S_{21} refer to the excitation of the fundamental mode at port 1.

		analytic model		simulation	
Waveguide radius	b	0.6 mm	0.48 mm	0.6 mm	0.48 mm
Radius of 1st bend	R_1	4.4 mm	1.953 mm	4.4 mm	1.92 mm
Angle of 1st bend	θ_1	43°	58°	43°	58°
Radius of 2nd bend	$\lvert R_2\rvert$	4.445 mm	2.348 mm	4.5 mm	2.25 mm
Angle of 2nd bend	$\lvert\theta_2\rvert$	133°	148°	133°	148°
Magnitude of TE_{11}	$\lvert S_{21}^{(TE)}\rvert$			−32.7 dB	−22.3 dB
Magnitude of TM_{01}	$\lvert S_{21}^{(TM)}\rvert$			−0.156 dB	−0.196 dB

Given a waveguide of radius b, with β_1 and β_2 being the imaginary parts of the propagation constants, $k = 2\pi/\lambda$ the vacuum wave number, the coupled mode equation of a general single bend with initial mode amplitudes $a_1 = A_1(0), a_2 = A_2(0)$ and radius of curvature R is solved by

$$A_1(z) = \left[a_1\left(\cos\frac{\pi z}{d'} + \eta\sin\frac{\pi z}{d'}\right) + a_2\eta\rho\sin\frac{\pi z}{d'}\right]e^{i\tilde{\beta}z}, \tag{1}$$

$$A_2(z) = \left[a_1\eta\rho\sin\frac{\pi z}{d'} + a_2\left(\cos\frac{\pi z}{d'} - \eta\sin\frac{\pi z}{d'}\right)\right]e^{i\tilde{\beta}z}, \tag{2}$$

$$\eta = \frac{i}{\sqrt{1+\rho'^2}}, \quad \tilde{\beta} = \frac{\beta_1+\beta_2}{2}, \tag{3}$$

where ρ and d are derived from the coupling coefficient,

$$\rho = -\frac{\beta_1+\beta_2}{\sqrt{2\beta_1\beta_2({u'_{11}}^2-1)({u'_{11}}^2-u_{01}^2)}}\frac{kb}{R}, \tag{4}$$

$$d = \frac{2\pi}{(\beta_1-\beta_2)\sqrt{1+\rho^2}}. \tag{5}$$

u_{01}, u'_{11} are the first roots of the zeroth Bessel function $J_0(z)$, and the derivative of the first Bessel function $J'_1(z)$.

Starting with the first bend of the converter, the amplitude evolution simplifies due to the initial values being $a_1 = 1, a_2 = 0$. In Eq. (4), the generic radius of curvature R is substituted by R_1. At $z^\star = R_1\theta_1$ the bend is inverted, implying $a_1 = A_1(z^\star), a_2 = A_2(z^\star)$ for the initial condition of the second bend with $R_2 < 0$. In Eqs. (1) and (2) the z-coordinate for the second bend must be given relative to the transition, substituting z with $z - z^\star$.

Two cases are studied with fixed waveguide radius. The first one is set to $b = 0.6\,\text{mm}$, which implies $\beta_1 = 5.487\,\text{mm}^{-1}, \beta_2 = 4.844\,\text{mm}^{-1}$ [16]. To achieve good conversion, $|A_1(\hat{z} = R_1\theta_1 + R_2\theta_2)|^2$ at the end of the second bend must be minimized. The coupling coefficients scale inversely with the radius of curvature [10], which results in strong coupling ($\rho \gg 1$) at $R_1 \approx \lambda$. However, moderate coupling $\rho \approx 1$ is beneficial with respect to broad bandwidth. $R_1 = 4.4\,\text{mm}$ is chosen as a good compromise ($\rho = 0.95$). The angle is adapted to achieve ≈50 % power in both modes at $z^\star$ according to Eqs. (1) and (2). θ_2 follows from the condition of a net 90° bend. Feeding the second bend with the superimposed amplitudes a_1 and a_2, the power $|A_2(\hat{z})|^2$ of mode 2 at the output port is optimized with respect to R_2. At the optimum the conversion reaches 99.97 %. Table 1 summarizes the structure parameters.

The second case considers a smaller waveguide of $b = 0.48\,\text{mm}$ with $\beta_1 = 4.981\,\text{mm}^{-1}$ and $\beta_2 = 3.799\,\text{mm}^{-1}$ due to potential excitation of TE_{21} enabled by manufacturing errors in the large waveguide. Following the same procedure the optimal geometric parameters are determined and listed in Table 1.

NUMERICAL VALIDATION AND REFINEMENT

To include finite conductivity, scattering parameters of the converters have been simulated in CST Studio Suite 2022 Microwave Studio [17]. Annealed copper is assumed as conductive wall, $\sigma_c = 58\,\text{MS m}^{-1}$.

For the large waveguide case, Fig. 2 shows how S_{21} evolves for both modes with varied radius of the second bend. For minimum transmission in TE_{11}, a slight shift of the ideal R_2 has been found in comparison to the analytic result, see Table 1. The simulation also quantifies of how much power is transmitted, converted and lost due to finite conductivity. Table 1 lists S_{21} for both modes. Transmission to the fundamental goes down to 0.05 % power. 96.5 % are transferred to the desired accelerating mode. The remaining 3.5 % are dominantly dissipated by ohmic losses. Further

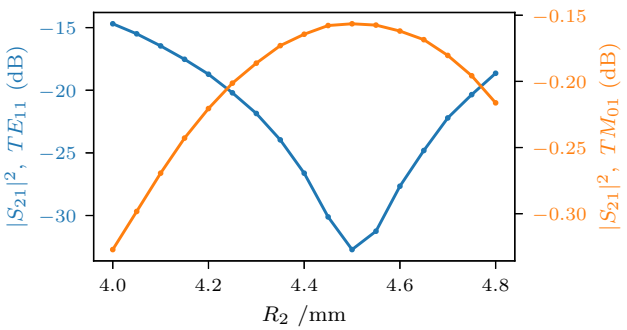

Figure 2: S_{21} of both modes versus radius of curvature R_2 for the large waveguide $b = 0.6\,\text{mm}$, and at 300 GHz.

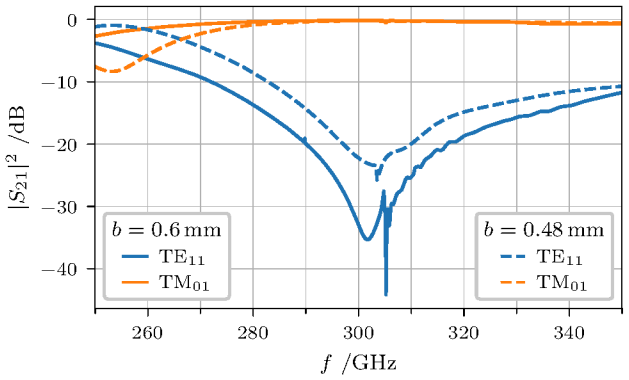

Figure 3: Scattering parameters $S_{21}^{(\mathrm{TM})}$ and $S_{21}^{(\mathrm{TE})}$ for the optimized hook-type mode converters. The design parameters are provided in Table 1.

validation and optimization has been applied to the small waveguide case, leading to the optimal structure parameters in Table 1.

Fig. 3 shows the frequency dependence of $S_{21}(f)$, stressing its broad bandwidth. Within its 3 dB–bandwidth, $\Delta f \approx 4$ GHz, the converter performs well with an unconverted transmission below the 1 ‰ level. The spike observed at 305 GHz is due to the cut-off frequency of the next higher order mode, TE_{21}. It is noticeable that $S_{21}^{(TE)}$ is still small in case of the small waveguide, but already an order of magnitude larger than for the $b = 0.6$ mm case.

PINHOLE FOR ELECTRON INJECTION

To inject an electron beam into the subsequent accelerating structure, a pinhole of radius r_p aligned with the outgoing waveguide axis is included in the computational model of the large waveguide. Substantial leakage of the field may occur at the pinhole, and mode conversion may deteriorate.

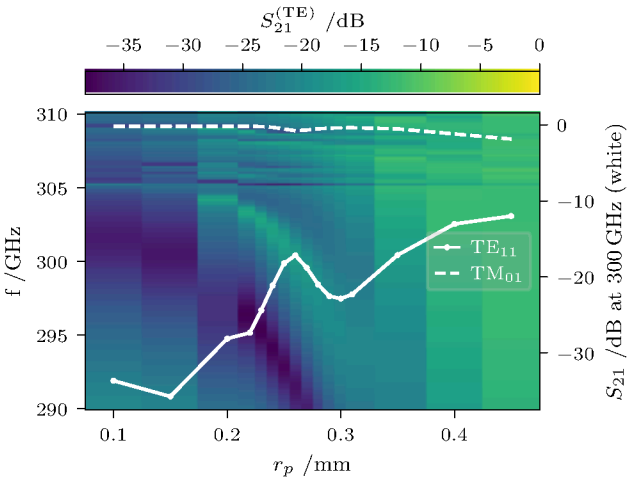

Figure 4: Transmissive $S_{21}^{(\mathrm{TE})}(f, r_p)$ in fundamental mode depending on frequency and pinhole radius r_p for beam injection. White line plots: $S_{21}^{(\mathrm{TE})}(r_p)$ and $S_{21}^{(\mathrm{TM})}(r_p)$ at 300 GHz.

Fig. 4 shows how the transmission in the fundamental mode changes with r_p. The resonance peak shifts towards smaller frequency as r_p increases, and $S_{21}^{(\mathrm{TE})}(300\,\mathrm{GHz})$ increases. With a 0.45 mm pinhole, conversion has dropped to 65 % and about ≈25 % of the power leaks out of the pinhole. In Fig. 5 the field pattern also makes potential leakage visible. For a small pinhole of 0.22 mm no significant leakage is observed, while for $r_p = 0.45$ mm a significant amount of field energy is localized at the opening. The clear TM_{01} field pattern at the output, shown in Fig. 5a, is heavily distorted in Fig. 5b. In conclusion, a pinhole of 0.22 mm is an acceptable trade-off between efficient mode conversion and sufficient space for beam injection.

CONCLUSION AND OUTLOOK

The double bend mode converter is a promising alternative to collinear coupling with a radially polarized Gaussian beam. Including losses due to linear-to-radial polarization conversion, the collinear scheme is expected to couple less efficiently to the accelerating mode than the waveguide-to-waveguide converter equipped with a conical horn antenna. Further, the hook-shaped structure supports the compactness of the accelerating structures. While an experimental layout for TM_{01}-horn-antenna coupling requires at minimum 50 mm (horn length and space for an in-coupling mirror), the hook-type converter requires less than 4 mm. Free space coupling is relocated from the beam axis to the surrounding. Due to its non-resonant characteristic, coupler kicks are expected to be negligible, but require further quantification in future studies.Further, the wall is modelled with 0.2 mm thickness in simulations. In practice, embedding the waveguide channel in a copper block may be beneficial, which may have an influence on the leakage at the pinhole.

ACKNOWLEDGEMENTS

The authors thank all the TWAC colleagues for fruitful discussions and input. The helpful feedback from MPY-1 colleagues was highly appreciated. Special thanks to F. Mayet for internal review of the manuscript.

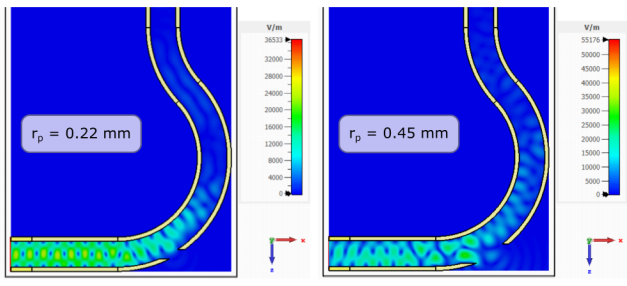

a b

Figure 5: Field pattern $|\mathbf{E}|$ of the two mode converters with (a) small and (b) large pinhole. The short pulse has left port 1 already and arrived at port 2. Parameters listed in Table 1.

REFERENCES

[1] E. A. Nanni *et al.*, "Terahertz-driven linear electron acceleration," *Nature Communications*, vol. 6, p. 8486, 2015. 10.1038/ncomms9486

[2] M. A. K. Othman *et al.*, "Experimental demonstration of externally driven millimeter-wave particle accelerator structure," *Applied Physics Letters*, vol. 117, no. 7, p. 073 502, 17, 2020. 10.1063/5.0011397

[3] M. T. Hibberd *et al.*, "Acceleration of relativistic beams using laser-generated terahertz pulses," *Nature Photonics*, vol. 14, no. 12, pp. 755–759, 10, 2020. 10.1038/s41566-020-0674-1

[4] F. X. Kärtner *et al.*, "AXSIS: Exploring the frontiers in attosecond X-ray science, imaging and spectroscopy," *Nuclear Instruments and Methods in Physics Research Section A: Accelerators, Spectrometers, Detectors and Associated Equipment*, vol. 829, pp. 24–29, 1, 2016. 10.1016/j.nima.2016.02.080

[5] C. Bruni *et al.*, "TWAC : EIC pathfinder open european project on novel dielectric acceleration," Venice, Italy, 2023. presented at IPAC'23, Venice, Italy, May 2023, paper TUPA061, this conference.

[6] T. Vinatier, R. W. Assmann, U. Dorda, F. Lemery, and B. Marchetti, "Simulation of a concept for a compact ultrafast X-ray pulse source based on RF and THz technologies," *Journal of Applied Physics*, vol. 125, no. 16, p. 164 901, 28, 2019. 10.1063/1.5091109

[7] M. Thumm, "High-power millimetre-wave mode converters in overmoded circular waveguides using periodic wall perturbations," *International Journal of Electronics*, vol. 57, no. 6, pp. 1225–1246, 1, 1984. 10.1080/00207218408938998

[8] H. Kumrić and M. Thumm, "Optimized overmoded TE01-to-TM11 mode converters for high-power millimeter wave applications at 70 and 140 GHz," *International Journal of Infrared and Millimeter Waves*, vol. 7, no. 10, pp. 1439–1463, 1, 1986. 10.1007/BF01010751

[9] H. Li and M. Thumm, "Mode conversion due to curvature in corrugated waveguides," *International Journal of Electronics*, vol. 71, no. 2, pp. 333–347, 1, 1991. 10.1080/00207219108925480

[10] D. V. Vinogradov and G. G. Denisov, "The conversion of waves in a bent waveguide with a variable curvature," *Radiophysics and Quantum Electronics*, vol. 33, no. 6, pp. 540–545, 1990. 10.1007/BF01037860

[11] L. Gen-Shen and Z. Jin-Juan, "Converters for the TE 11 Mode Generation from TM 01 Vircator at 4 GHz," *Chinese Physics Letters*, vol. 18, no. 9, pp. 1285–1287, 2001. 10.1088/0256-307X/18/9/342

[12] G. G. Denisov and M. L. Kulygin, "Numerical Simulation of a TM01–TE11 Waveguide Mode Converter by the FDTD Method," *Radiophysics and Quantum Electronics*, vol. 48, no. 3, pp. 185–194, 2005. 10.1007/s11141-005-0059-9

[13] G. Chen, T. Katagiri, H. Song, N. Yusa, and H. Hashizume, "Detection of cracks with arbitrary orientations in a metal pipe using linearly-polarized circular TE11 mode microwaves," *NDT & E International*, vol. 107, p. 102 125, 2019. 10.1016/j.ndteint.2019.102125

[14] E. A. Nanni, M. D. Forno, V. A. Dolgashev, J. Neilson, and S. G. Tantawi, "Mm-Wave Standing-Wave Accelerating Structures for High-Gradient Tests," in *Proc. IPAC'16*, 2016, pp. 3884–3887. 10.18429/JACoW-IPAC2016-THPOR044

[15] E. A. Nanni *et al.*, "Prototyping high-gradient mm-wave accelerating structures," *Journal of Physics: Conference Series*, vol. 874, p. 012 039, 2017. 10.1088/1742-6596/874/1/012039

[16] D. M. Pozar, "Circular Waveguide," in *Microwave Engineering*, 2011, pp. 121–130.

[17] *CST Studio Suite 3D EM simulation and analysis software*, version 2022, Dassault Systèmes, 2022. https://www.3ds.com/products-services/simulia/products/cst-studio-suite/